Available online at www.sciencedirect.com
SCIENCE DIRECT®
Journal of Power Sources 119–121 (2003) 522–527
JOURNAL OF POWER SOURCES
www.elsevier.com/locate/jpowsour

Electrochemically lithiated graphite characterised by photoelectron spectroscopy

A.M. Andersson[a], A. Henningson[b], H. Siegbahn[b], U. Jansson[a], K. Edström[a,*]

[a]*Department of Materials Chemistry, Ångström Laboratory, Uppsala University, Box 531, SE-751 21 Uppsala, Sweden*
[b]*Department of Physics, Ångström Laboratory, Uppsala University, Box 530, SE-751 21, Uppsala, Sweden*

Abstract

X-ray photoelectron spectroscopy (XPS) has been used to study the depth profile of the solid–electrolyte interphase (SEI) formed on a graphite powder electrode in a Li-ion battery. The morphology of the SEI-layer, formed in a 1 M $LiBF_4$ EC/DMC 2:1 solution, consists of a 900 Å porous layer of polymers (polyethylene oxide) and a 15–20 Å thin layer of Li_2CO_3 and $LiBF_4$ reduction–decomposition products. Embedded LiF crystals as large as 0.2 μm were found in the polymer matrix. LiOH and Li_2O are not major components on the surface but rather found as a consequence of sputter-related reactions. Monochromatised Al Kα XPS-analysis based on the calibration of Ar^+ ion sputtering of model compounds combined with a depth profile analysis based on energy tuning of synchrotron XPS can describe the highly complex composition and morphology of the SEI-layer.

Keywords: X-ray photoelectron spectroscopy; Electrochemically lithiated graphite; SEI; Depth profile analysis

1. Introduction

It is well established that a solid–electrolyte interphase (SEI) form, on the surface of a carbon electrode in a Li-ion cell at ∼0.8 V versus Li/Li^+ during the first charge (Li-intercalation) [1–3]. The chemical composition of this SEI-layer forming in carbonate-based electrolytes has been evaluated, mainly by Fourier transform–infrared (FT–IR) spectroscopy, and comprises species like Li_2CO_3, $ROCO_2Li$, lithium alkoxides, Li_2O, LiF, LiCl and purely organic or polymeric compounds [3]. Several models have been proposed for the spatial organisation of these phases on the electrode surface. Aurbach and Zaban modelled impedance data describing the formation of a sub-layer in a multi-layer structure [4,5]. Peled et al. [6] suggested a more complex model of a mosaic type SEI with at least three RC elements representing each sub-layer, emphasising the resistance of grain boundaries between the micro-phases within the SEI. Modelling of the total film thickness from impedance data has given values from 10–50 Å [5]. Other studies have shown very varying results. In situ ellipsometry measurements on a highly oriented pyrolytic graphite (HOPG) crystal have given a value of 40 Å [7], while studies by in situ electrochemical atomic force microscopy (ECAFM) have suggested surface deposits in the order of 250 Å to several thousands Ångström (Å) thick [8–10]. These studies and other in situ ECAFM studies have also reported a heterogeneous, non-uniform film with a rough hill-like structure [11], while most XPS studies have assumed a macroscopically smooth layer with one specific thickness [12–14]. The morphological studies performed on carbon have been restricted to the use of HOPG, which can be regarded as a model system and, hence do not give an accurate picture of the situation in a real battery system.

X-ray photoelectron spectroscopy (XPS) is a highly useful method for studying the surface chemistry of electrode materials because of its surface sensitivity (<30 Å). In particular, qualitative and quantitative information relating to the SEI formed on lithium metal and carbon-based anodes has been successfully obtained in several studies [12–21]. Unlike FT–IR spectroscopy, all species that are present in measurable amounts (>1%) can be detected. Depth profiling of the sample surface can provide useful information on the morphological features. This can be achieved by Ar^+-ion etching (sputtering) of the surface, followed by XPS analysis. To obtain a reliable depth scale, calibration of the sputtering rate is required [22]. Also, the topography and changes of surface composition due to ion beam-induced damages have to be taken into account in the depth profile calibration. Depth profiling by XPS can also be achieved by using synchrotron radiation [23]. By tuning the X-ray

* Corresponding author.
E-mail address: kristina.edstrom@mkem.uu.se (K. Edström).

0378-7753/03/$ – see front matter
doi:10.1016/S0378-7753(03)00277-5

energy, the escape depth of the photoelectron can be changed and, hence also the sampling depth. A shallower depth interval, complementary to the conventional Mg Kα or Al Kα XPS analysis/sputtering technique, can hereby be probed. The technique is, in addition, non-destructive and does not restrict the analysis sensitivity of photoelectrons with low binding energy (for example, Li).

In this study, the use of XPS analysis of the SEI-layer formed on a graphite electrode in a real battery configuration will be explored. The purpose is to describe in detail the chemical composition and morphology of the SEI-layer as a function of depth. A second goal is to determine SEI-layer thickness as well as understand the influence of Ar^+ ion sputtering on the chemical composition of the SEI-layer.

2. Experimental

Carbon electrodes were prepared by spreading a mixture of 95 wt.% Timrex KS6 (Timcal A + G, Sins, Switzerland), and 5 wt.% EPDM rubber binder in cyclohexane onto a porous Cu foil current collector (Metfoil AB, Sweden). Our preparation of ⟨Lil1 M $LiBF_4$ (Battery grade, Tomiyama) in ethylene carbonate (EC)/dimethyl carbonate (DMC, 2:1, Selectipur®, Merck)lgraphite⟩ electrodes have been described in detail in [20]. The water content in the electrolyte was determined by Karl Fischer titration to ca. 10–20 ppm. The cell laminates were packed in polymer-coated aluminium bags, evacuated and sealed. All preparations were conducted in an Ar-filled glove-box (H_2O, $O_2 < 3$ ppm).

The cells were cycled galvanostatically at a *C*/7 rate (∼0.05 mA/cm^2). The cycling was conducted between 0.01 and 1.5 V, and interrupted after two cycles at either the low cut-off voltage when the graphite was in its fully intercalated state or at the high cut-off voltage for the de-intercalated state. Small pieces of the electrode were cut-out in the glove-box and attached to a sample holder. The samples were not washed prior to the measurements to ensure that no material on the surface was dissolved in the washing solvent. This is reflected in the spectra by the presence of electrolyte salt peaks, which can be easily identified and separated from the signals from the other surface components. The samples were transported to the spectrometer in a sample holder preventing exposure to air and moisture.

The XPS measurements were conducted on a laboratory spectrometer (Phi 5500) using monochromatised Al Kα radiation (1486.6 eV). Absolute binding energies are slightly higher than that given in literature due to non-uniform charging effects of non-conducting micro-domains of salt residuals and reduction products on the surface. They can, hence, not be used directly for chemical analysis of the spectra. Internal references have to be used and reference measurements on compounds present on the surface were performed, and from the relative peak positions (binding energy differences) and relative intensities, a majority of peaks in the spectra could be assigned. The reference compounds were: $LiBF_4$ (Tomiyama), Li_2CO_3 (Merck), LiF (Crystal) and CH_3OLi (Merck) and polyethylene oxide (PEO, Merck), highly oriented pyrolytic graphite (HOPG, Advanced Ceramics Corporation) and chemically lithiated HOPG. The lithiated sample was synthesised by immersing a piece of HOPG into a Li metal melt at 280 °C for 48 h. The HOPG crystals were cleaved prior to the measurements to obtain a fresh surface. The energy scale was adjusted based on the graphite peak in the C 1s spectrum at 284.3 eV. A depth profile was obtained by Ar^+ ion beam sputtering (4 keV). The sputtering rate was determined for the four major components: graphite, Li_2CO_3, polymeric hydrocarbon (polyethylene oxide) and LiF. This was achieved by sputtering followed by profilometer measurements on pressed-pellet or thin film samples of the compounds. Peak-fit analysis was performed on all the spectra using Gaussian–Lorenzian peak shapes and Shirley background correction. Quantitative information of surface composition was obtained from integrated peak intensities and atomic sensitivity factors from the PHI software [24].

Efforts were undertaken to minimise the amount of absorption of contaminants on the electrode surface. Despite this, there will always be species like water, hydroxyls and electrolyte residue sticking to the surface, which are not part of the electrochemically formed SEI-layer. The extent of contaminant absorption was estimated by analysing an electrode dipped into electrolyte by XPS. The same procedure was used for a LiF reference sample, since LiF is a major SEI-layer component and its ionic character is different from graphite.

Photoelectron spectra were also obtained at beam line 411 at the Swedish National Synchrotron Radiation Laboratory MAX. The samples were transported to the synchrotron facility in vacuum-sealed polymer-coated aluminium bags. They were unpacked in an Ar-filled glove-box (<1 ppm H_2O) and mounted on a sample holder with an o-ring sealed protection tube. The sample holder was attached to the manipulator rod on the spectrometer, and the protection tube was removed under vacuum. The energy scale was calibrated versus Fermi level via measurement of the Fermi edge of the spectrum.

3. Results and discussion

3.1. SEI-layer composition as determined by conventional XPS

The SEI-layer formed on the graphite surface, as determined by conventional XPS (see Fig. 1), was shown to comprise solvent reduction products ($ROCO_2Li$), polymeric species (hydrocarbons and possibly polyethylene oxide) and $LiBF_4$ reduction or decomposition products (LiF and $Li_xBO_yF_z$) (Table 1). A detailed description of the peak assignment procedure is found in [25]. The results are in line with

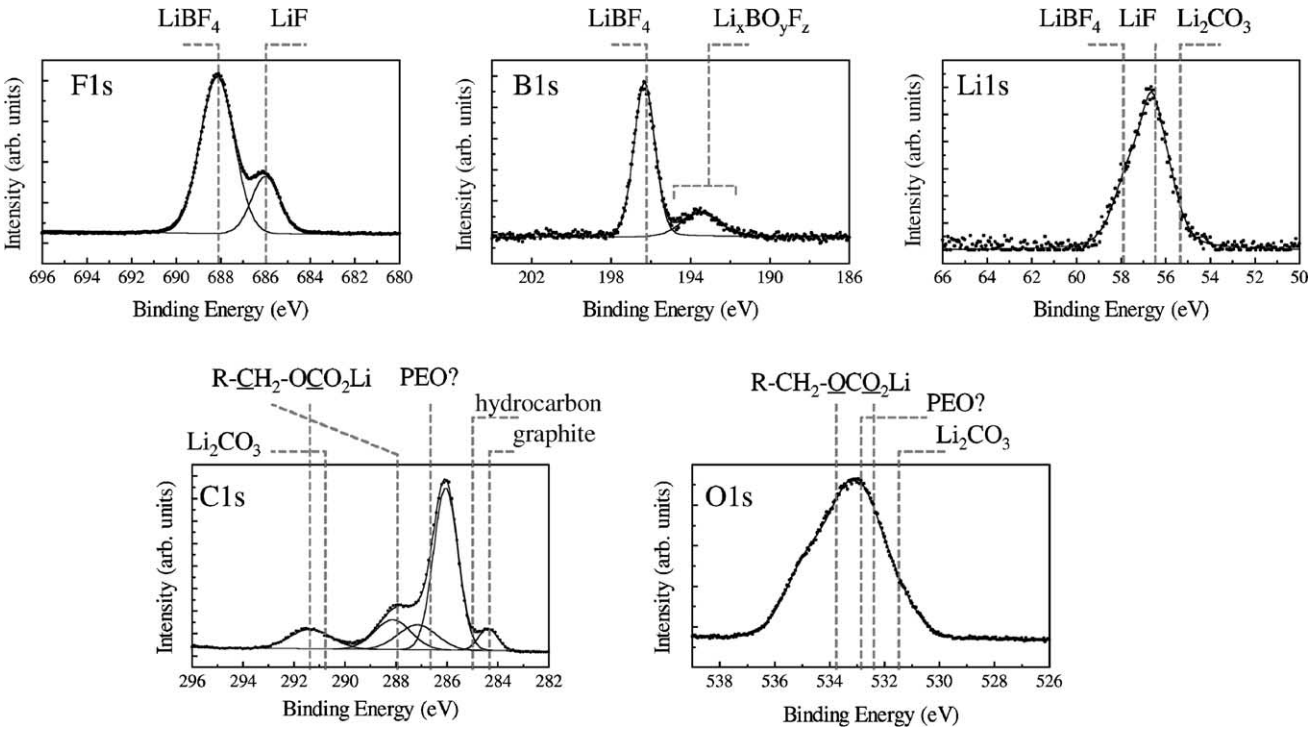

Fig. 1. F 1s, B 1s, Li 1s, C 1s and O 1s XPS spectra for a de-intercalated graphite electrode after two cycles in EC/DMC, 1 M $LiBF_4$. Binding energy positions from reference compound measurements are marked in the figures.

previous results obtained for carbon electrodes cycled in this electrolyte [3–6,17,20,26].

The extent of contamination measured on graphite and LiF dipped into electrolyte shows that a very small amount of surface species absorbs on the non-polar graphite surface. More species are absorbed on the polar LiF sample. The majority of the carbon present on the surface is present as hydrocarbons and only a minor amount of oxygen-containing species is observed. It can hence be concluded that a majority of the oxygen-containing species observed for the cycled sample (i.e. carbonates) is indeed due to electrochemically formed compounds. All surface species on the dipped samples were removed within 30 s of sputtering.

3.2. Depth profile information

The new information regarding SEI-morphology gained in this study lies in the depth profile results using Ar^+ ion sputtering and energy-tuned synchrotron XPS.

Removing material from a surface by Ar^+ ion sputtering is highly abusive and can cause sputtering-induced roughness, preferential removal of some element and decomposition of compounds. The various effects of sputtering on compounds relevant to the electrode measurements were, therefore, analysed individually. One important result is the formation of Li_2O as a consequence of Li_2CO_3 decomposition. Sputtering of LiF, graphite and polyethylene oxide did

Table 1
The XPS peak assignments in this study

Assigned compound	Measured binding energy (eV)					Reference binding energy difference (eV)[a]		
	C	O	Li	F	B	Δ(C–O)	Δ(Li–F)	Δ(F–B)
Graphite	284.3							
Hydrocarbon	285							
PEO (ether)	286.5	533				246.3		
Li_2CO_3	290	532	55.5			241.8		
R–CH_2OCO_2Li[b]	290–291	532.5						
R–CH_2OCO_2Li[b]	288	534						
LiF			56.5	686			629.3	
$LiBF_4$			58	688.2	196.3		630.3	491.8

[a] Refers to values obtained from reference compound measurements.
[b] Approximate values obtained from [24].

not affect the material in any way while $LiBF_4$ decomposed forming small amounts of LiF. Intercalated LiC_6 electrode was not stable during sputtering causing LiOH to precipitate on the surface.

The sputtered samples were scanned in a profilometer to obtain the individual sputtering rates. The results show a slower sputtering rate for the inorganic salts compared to the organic compounds. They are all in the same range, showing that preferential removal of material should not be a critical issue for the measurements on the cycled electrodes. A detailed description is found in [25].

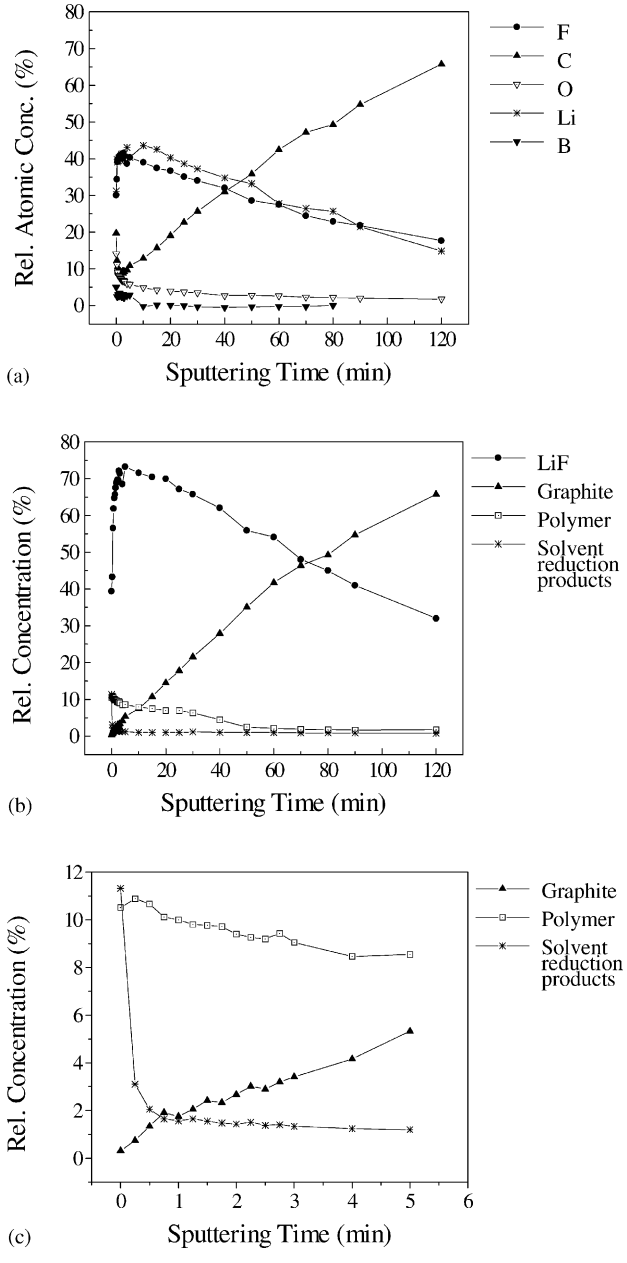

Fig. 2. Sputtering analysis of a graphite electrode after two cycles in EC/DMC, 1 M LiBF4, visualised as: (a) atomic fraction as a function of sputtering time, (b) molar fractions of graphite, solvent reduction products (SPR), polymers, LiF and $LiBF_4$, on the graphite electrode surface as a function of sputtering time, and (c) an enlarged image of (b).

The sputtering results of the electrochemically cycled electrodes, based on both peak assignments and the sputtering calibration, are summarised in a quantitative way in Fig. 2, where the relative concentration of the major surface species are given as a function of sputtering time. Using the sputtering time needed to obtain half the original signal intensity for a certain compound and its sputter rate, one can obtain an estimate of the film thickness. Here, the data shows a fast exponential decay of the carbonate (solvent reduction products) signal, where half of the levelling-out time is ca. 30 s. This corresponds to a thickness of <20 Å, according to the sputtering rate determined for Li_2CO_3. The polymer phase signal is instead fairly constant for about 35 min, and then levels out quickly. This shows that the organic polymers are distributed within a thicker layer (up to 900 Å). The LiF shows a maximum of ca. 70%, and then decreases linearly. This is consistent with a surface containing LiF crystals of various sizes with a maximum size of ∼0.2 μm. These crystals and their sizes are also possible to detect with SEM (Fig. 3). Rinsing the electrode in DMC, which does not dissolve LiF, diminished the amount by more than half. Most of the LiF appears, therefore, on the surface as more or less loosely attached crystals rather than an integrated part of the surface layer.

LiOH has been reported to form a thick layer close to the graphite surface [12]. Here, it only occurred occasionally in the spectra from a number of de-intercalated electrodes, and we believe that its presence is rather a consequence of sputter-related reactions, for example, re-deposition of sputtered samples on the surface. LiOH and Li_2O are hence not major components of the SEI-layer.

The synchrotron radiation excitation was used on both de-intercalated and fully intercalated electrodes. In our experiments, the photon energy was varied between 454 and 1061 eV, which corresponds to a variation in sampling depth in the range of 5–20 Å [27].

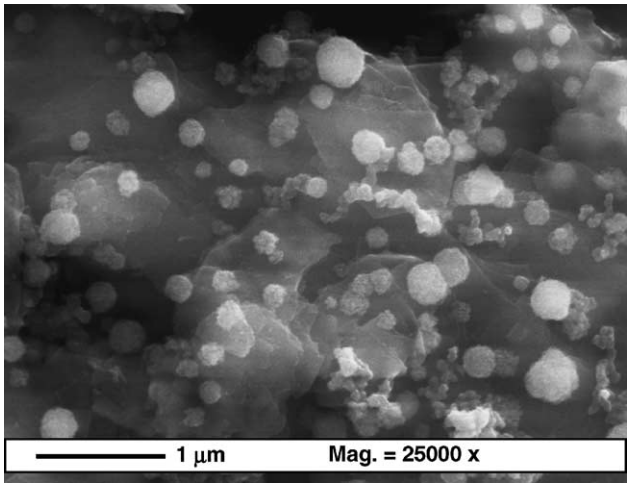

Fig. 3. An SEM micrograph of a KS6 graphite electrode galvanostatically cycled three times at *C*/5 in EC/DMC, 1 M $LiBF_4$ electrolyte.

The measurement showed peak intensity variations in the above given photon energy range, indicating a micro-structural ordering within the outermost surface layer. In particular, the near-disappearance of the graphite C 1s peak at 284.5 eV for the 454 eV photon energy (Fig. 4) shows that the SEI-layer completely covers the graphite surface. Based on the empirical relationship between the escape depth of a photoelectron and its kinetic energy and the matrix within which it travels toward the surface [27,28], these results are consistent with a minimum layer thickness of 15–20 Å. In the spectrum taken at 454 eV, there are, aside from the main hydrocarbon peak, two shoulders visible around 288 and 290.5 eV. These are due to ether and carbonate carbons, respectively. Little or no signal from the underlying graphite is visible in this spectrum, proving the SEI-layer to totally cover the graphite surface. The spectra taken at photon energies of 758 and 1061 eV are similar to the 454 eV spectrum, the main difference being the growing graphite peak at 284.3 eV. In the Al Kα excited spectrum at 1486 eV, this peak increases even further. The C 1s spectra for the lithiated electrode are shown in Fig. 4. The features due to hydrocarbon, ether and carbonate species have closely the same relative positions as in the de-intercalated sample. The overall shift of 1.6 eV is due to the different work functions for the intercalated and de-intercalated samples [29]. The relative intensity of the graphite peak is substantially smaller in these spectra, implying a thicker layer in this case. Based on estimation of the escape depth as described in [25], the observed graphite C 1s intensity variation for the de-intercalated sample is consistent with a minimum layer thickness of around 15–20 Å.

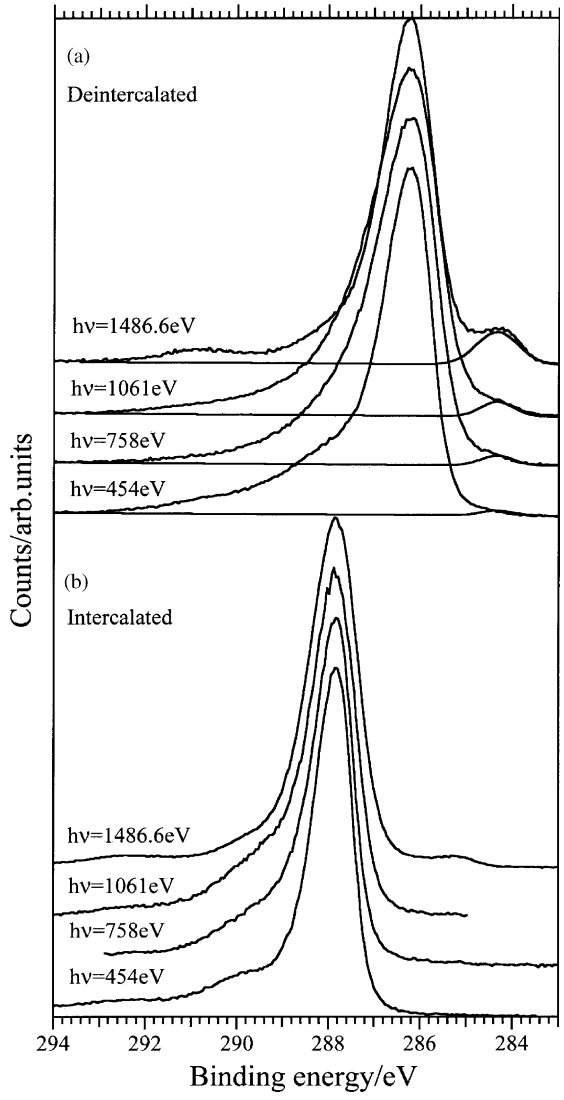

Fig. 4. Synchrotron radiation excited C 1s spectra for cycled graphite electrodes in their: (a) de-intercalated, and (b) intercalated states. Spectra were taken at photon energies of 454, 758, 1061 eV and were calibrated vs. Fermi edge for each sample. The 1486.6 eV spectrum was excited with Al Kα radiation.

The combination of two XPS techniques is useful for achieving both compositional and morphological information on the SEI formed on a graphite electrode, suitable for a true Li-ion battery. Both the methods describe a 15–20-thick layer containing Li_2CO_3 and reduction or decomposition products of $LiBF_4$. Depth analysis by Ar^+ ion sputtering showed that it could cause decomposition of unstable surface species (e.g. formation of Li_2O and LiOH from Li_2CO_3), a knowledge not accounted for in previous studies of SEI-layers. A depth profile of the electrode surface in the interval ∼20–2000 Å was carried out by peak assignment and calibration of the effect of sputtering, describing that large crystals of ∼0.2 μm LiF were found distributed in a 900 Å-thick polymer matrix of mainly polyethylene oxide. These results support the notion that the SEI-layer has a highly irregular morphology.

Acknowledgements

This work was supported by grants from The Swedish Science Research Council (VR) and The Nordic Energy Research Programme (NERP).

References

[1] E. Peled, J. Electrochem. Soc. 126 (1979) 2047.
[2] P. Arora, R.E. White, M. Doyle, J. Electrochem. Soc. 145 (1998) 3647.
[3] D. Aurbach, Nonaqueous Electrochemistry, Marcel Dekker, New York, 1999.
[4] D. Aurbach, A. Zaban, J. Electroanal. Chem. 348 (1993) 155.
[5] A. Zaban, D. Aurbach, J. Power Sources 54 (1995) 289.
[6] E. Peled, D. Golodnitsky, G. Ardel, J. Electrochem. Soc. 144 (1997) L208.
[7] F. Kong, J. Kim, X. Song, M. Inaba, K. Kinoshita, F. McLarnon, Electrochem. Solid State Lett. 1 (1998) 39.
[8] A.C. Chu, J.Y. Josefowicz, G.C. Farrington, J. Electrochem. Soc. 144 (1998) 4161.
[9] K. Hirasawa, T. Sato, H. Asahina, S. Yamagushi, S. Mori, J. Electrochem. Soc. 144 (1997) 481.

[10] D. Alliata, R. Kötz, P. Novak, H. Siegthaler, Electrochem. Commun. 6 (2000) 436.
[11] S. Geniès, R. Yazami, H. Estrade-Schwarekopf, B. Rousseau, ITE Battery Lett. 1 (1995) 15.
[12] K. Kanamura, S. Shiraishi, H. Takezawa, Z. Takehara, Chem. Mater. 9 (1997) 1797.
[13] S. Shiraishi, K. Kanamura, Z. Takehara, Langmuir 13 (1997) 3542.
[14] A. Schechter, D. Aurbach, H. Cohen, Langmuir 15 (1999) 3334.
[15] K. Kanamura, H. Tamura, Z. Takehara, J. Electroanal. Chem. 333 (1992) 127.
[16] K. Kanamura, H. Tamura, S. Shiraishi, Z. Takehara, J. Electrochem. Soc. 142 (1995) 340.
[17] A.M. Andersson, K. Edström, J.O. Thomas, J. Power Sources 81–82 (1999) 8.
[18] A.M. Andersson, K. Edström, Å. Wendsjö, N. Rao, J. Power Sources 81–82 (1999) 287.
[19] K. Edström, M. Herranen, J. Electrochem. Soc. 147 (2000) 3628.
[20] A.M. Andersson, K. Edström, J. Electrochem. Soc. 148 (2001) A1100.
[21] A.M. Andersson, M. Herstedt, A. Bishop, K. Edström, Electrochim. Acta 47 (2002) 1885.
[22] R. Smith, J.M. Walls, in: J.M. Walls (Ed.), Methods of Surface Analysis, Cambridge University Press, Cambridge, 1989, p. 20.
[23] H. Shimada, N. Matsubayashi, M. Imamura, T. Sato, A. Nishijima, Appl. Surf. Sci. 100–101 (1996) 56.
[24] C. Wagner, W. Riggs, L. Davis, J. Moulder, G. Muilenbery, Handbook of X-ray Photoelectron Spectroscopy, Perkin-Elmer Corp., Physical Electronics Division, Eden Prairie, MN, 1979.
[25] A. Andersson, Surface phenomena in lithium batteries, Ph.D. Thesis, Acta Universitatis Upsaliensis 656 (2001) (http://publications.uu.se/theses/).
[26] E. Peled, D. Bar Tow, A. Merson, A. Gladkichm, L. Burstein, D. Golodnitsky, J. Power Sources 97–98 (2001) 52.
[27] C.L.A. Lamont, J. Wilkes, Langmuir 15 (1999) 2037.
[28] D. Briggs, M.P. Seah, Practical Surface Analysis, Wiley, Chichester, 1983.
[29] G.K. Wertheim, P.M.Th.M. Van Attekum, S. Basu, Solid State Commun. 33 (1980) 1127.